NSTAR 2017

ω (782) Electroproduction in the Resonance Region

Research supported in part by the National Science Foundation under Grant No. 0856010 and the Jefferson Science Associates/Jefferson Lab Graduate Fellowship Program.

Evan Phelps

Department of Physics and Astronomy
University of South Carolina

UNIVERSITY OF SOUTH CAROLINA

Jefferson Lab

clas

Context

The talks of NSTAR 2017 have provided rich theoretical, experimental, and historical context.

QCD **unified** crucial aspects of disparate lines of evidence:

- quarks and color (Gell-Mann),
- partons and scaling (SLAC experiments), and
- QFT and renormalization,

BUT even today **critically lacks**

- the simplest bound-state solutions and
- a clear connection to its own dynamical properties.

So, what do we do?

- Study physical objects that encode QCD dynamics.

Probing the proton with ω

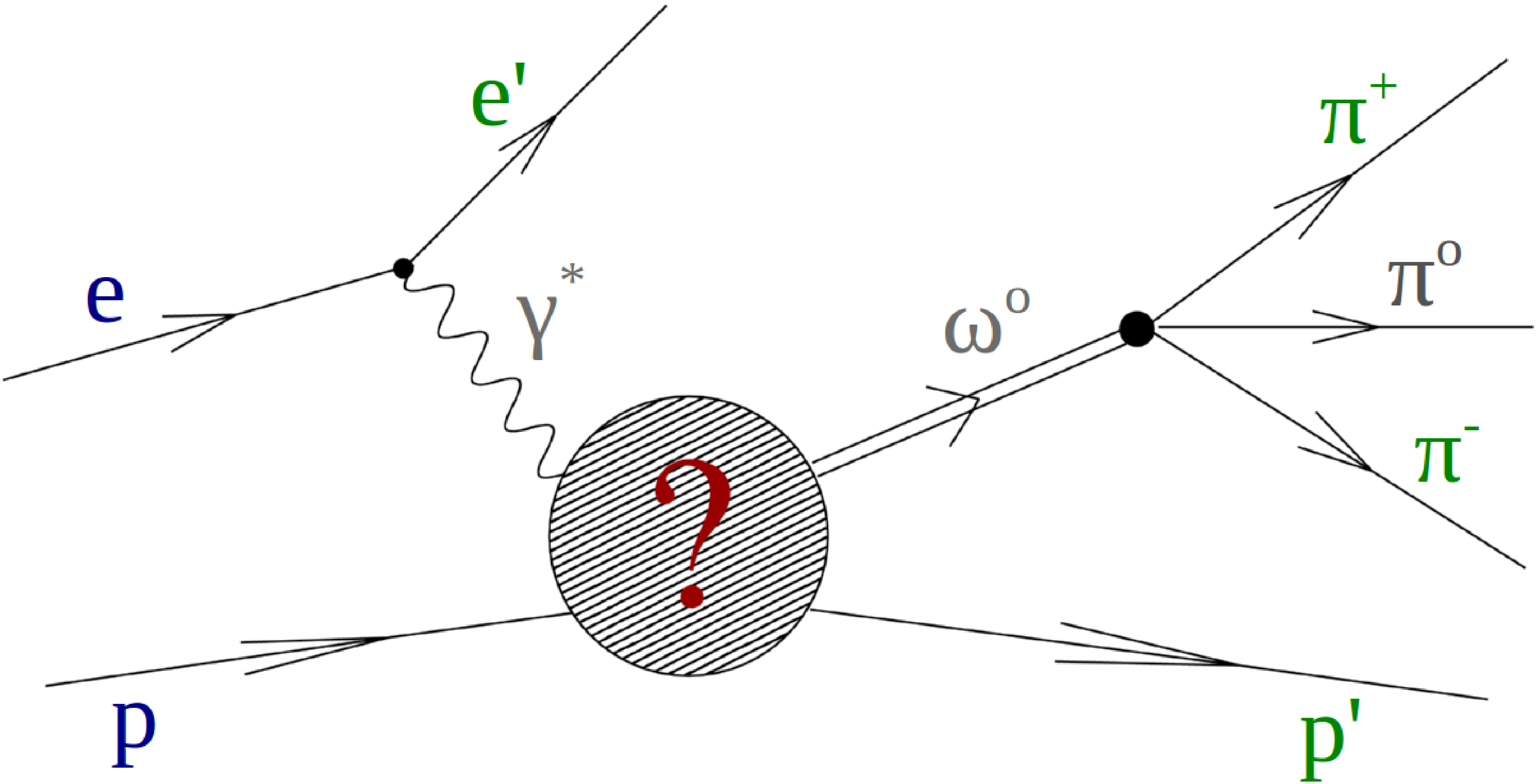

$ep \rightarrow e'\omega^o p' \longrightarrow \gamma^* p \rightarrow \omega^o p' \longrightarrow \pi^+\pi^o\pi^- p'$

Probing the proton with ω

- ω is selective,
  - isoscalar so couples only to I = ½ excited states
  - decays into 3π so filters out lower lying resonances
- might couple more strongly to states previously undetected in π production, and
- could corroborate available $\gamma^{*}pN^{*}$ information in exclusive channel with different background.

Particle	J^P	overall	πN	γN	$N\eta$	$N\sigma$	$N\omega$
N	$1/2^+$	****					
$N(1440)$	$1/2^+$	****	****	****		***	
$N(1520)$	$3/2^-$	****	****	****	***		
$N(1535)$	$1/2^-$	****	****	****	****		
$N(1650)$	$1/2^-$	****	****	***	***		
$N(1675)$	$5/2^-$	****	****	***	*		
$N(1680)$	$5/2^+$	****	****	****	*	**	
$N(1685)$	$?^?$	*					
$N(1700)$	$3/2^-$	***	***	**	*		
$N(1710)$	$1/2^+$	***	***	***	***		**
$N(1720)$	$3/2^+$	****	****	***	***		
$N(1860)$	$5/2^+$	**	**				
$N(1875)$	$3/2^-$	***	*	***			**
$N(1880)$	$1/2^+$	**	*	*		**	
$N(1895)$	$1/2^-$	**	*	**	**		
$N(1900)$	$3/2^+$	***	**	***	**		**
$N(1990)$	$7/2^+$	**	**	**			
$N(2000)$	$5/2^+$	**	*	**	**		
$N(2040)$	$3/2^+$	*					
$N(2060)$	$5/2^-$	**	**	**	*		
$N(2100)$	$1/2^+$	*					
$N(2150)$	$3/2^-$	**	**	**			
$N(2190)$	$7/2^-$	****	****	***			*
$N(2220)$	$9/2^+$	****	****				
$N(2250)$	$9/2^-$	****	****				
$N(2600)$	$11/2^-$	***	***				
$N(2700)$	$13/2^+$	**	**				

Probing the proton with ω

- Sensitive to N(2000) $5/2^+$?

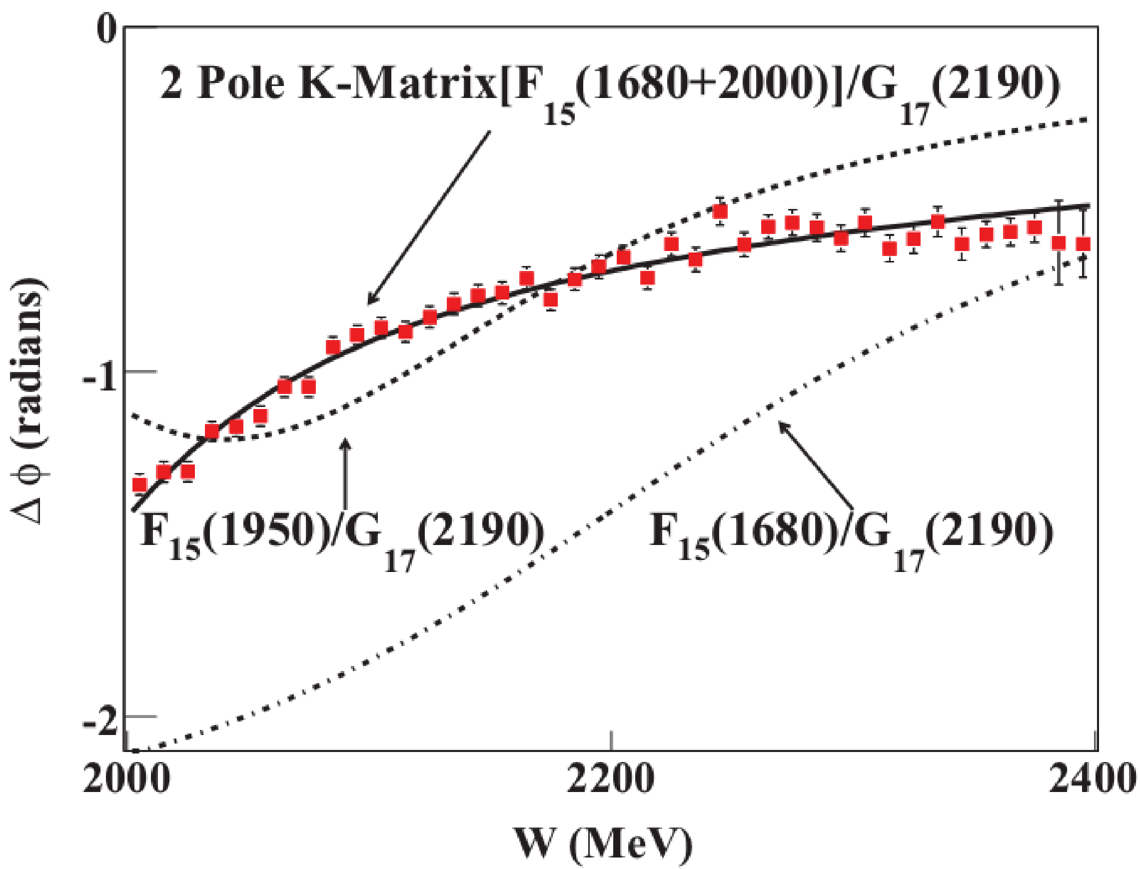

M. Williams et al., *Partial wave analysis of the reaction γp → pω and the search for nucleon resonances*, Phys. Rev. C 80 (2009), 065209.

arXiv:0908.2911v3

Particle	J^P	overall	πN	γN	$N\eta$	$N\sigma$	$N\omega$
N	$1/2^+$	****					
$N(1440)$	$1/2^+$	****	****	****		***	
$N(1520)$	$3/2^-$	****	****	****	***		
$N(1535)$	$1/2^-$	****	****	****	****		
$N(1650)$	$1/2^-$	****	****	***	***		
$N(1675)$	$5/2^-$	****	****	***	*		
$N(1680)$	$5/2^+$	****	****	****	*	**	
$N(1685)$	??	*					
$N(1700)$	$3/2^-$	***	***	**	*		
$N(1710)$	$1/2^+$	***	***	***	***		**
$N(1720)$	$3/2^+$	****	****	***	***		
$N(1860)$	$5/2^+$	**	**				
$N(1875)$	$3/2^-$	***	*	***			**
$N(1880)$	$1/2^+$	**	*	*		**	
$N(1895)$	$1/2^-$	**	*	**	**		
$N(1900)$	$3/2^+$	***	**	***	**		**
$N(1990)$	$7/2^+$	**	**	**			
$N(2000)$	$5/2^+$	**	*	**	**		
$N(2040)$	$3/2^+$	*					
$N(2060)$	$5/2^-$	**	**	**	*		
$N(2100)$	$1/2^+$	*					
$N(2150)$	$3/2^-$	**	**	**			
$N(2190)$	$7/2^-$	****	****	***			*
$N(2220)$	$9/2^+$	****	****				
$N(2250)$	$9/2^-$	****	****				
$N(2600)$	$11/2^-$	***	***				
$N(2700)$	$13/2^+$	**	**				

Kinematics and Observables

16	kinematic d.o.f.
-4	E p_x p_y p_z conservation
-4	initial proton at rest
-2	$q_x = q_y = 0$
-2	fixed m_ω and m_p
-1	azimuthal symmetry
3 **+1**	**kinematic variables** ***W*** or x_b, Q^2, and $\cos\theta^*$ or t' ... plus φ^* for **dynamics**

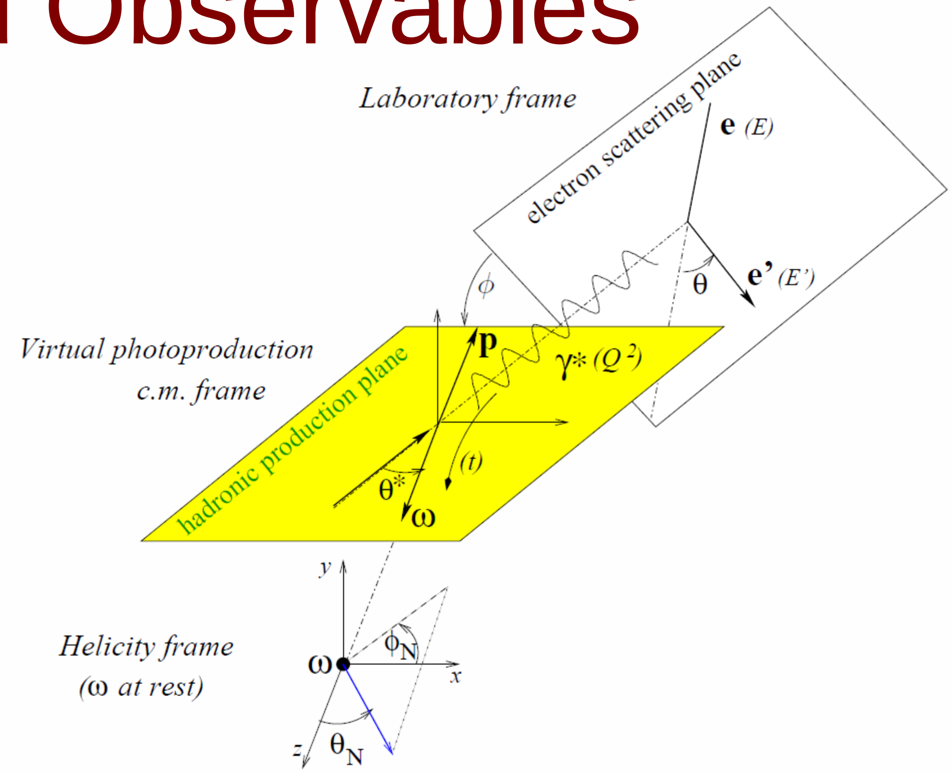

$$\frac{d^4\sigma}{dW \cdot dQ^2 \cdot d\Omega^\star} = \frac{1}{L} \cdot \frac{\Delta N}{\Delta W \cdot \Delta Q^2 \cdot \Delta\Omega^\star} = \Gamma_v \frac{d^2\sigma}{d\Omega^\star}$$

36	helicity amplitudes
-18	parity/time-reversal
324	$(=18^2)$ bilinear covariants
36	real parameters
-1	overall phase invariance
minimum of **35**	**real parameters required for complete description**

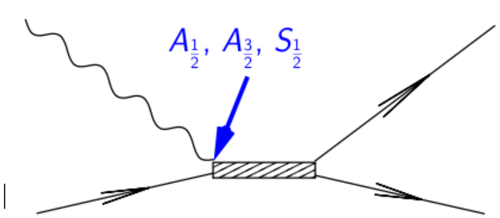

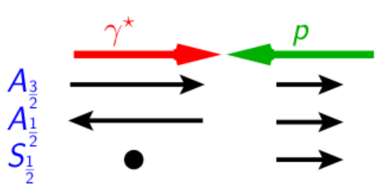

Kinematics and observables

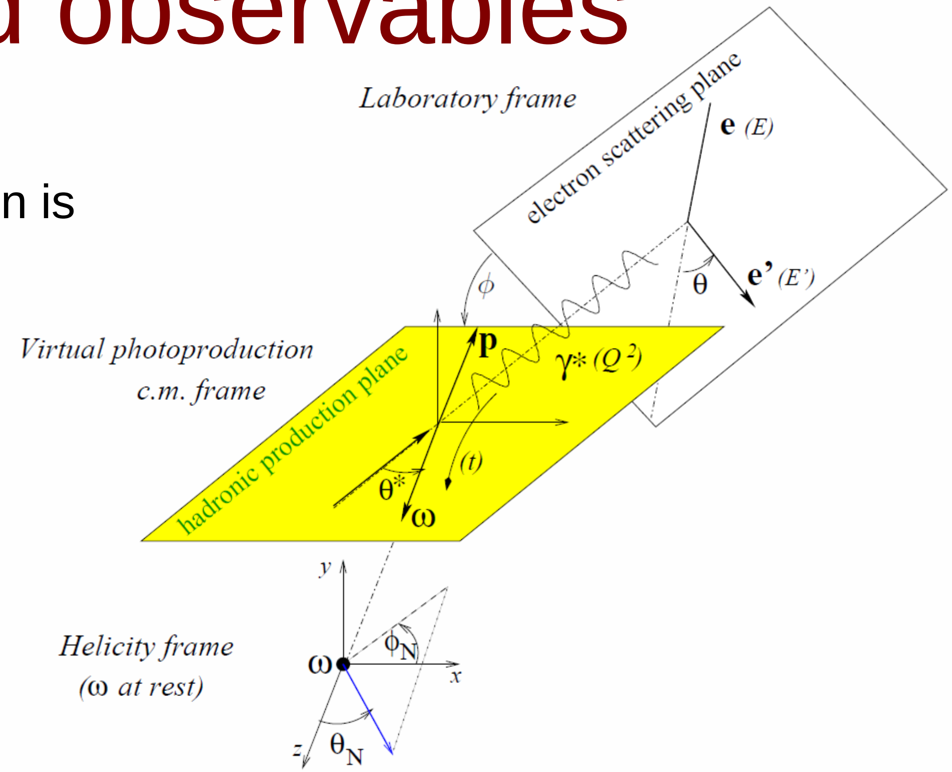

Measured ep scattering exclusive cross-section is reduced to γ*p→ωp exclusive cross-section:

$$\frac{d^4\sigma}{dW\,dQ^2\,d\Omega^*} = \Gamma\frac{d^2\sigma_h}{d\Omega^*}$$

and decomposed into response functions:

$$\frac{d^2\sigma_h}{d\Omega^*} = \frac{|\vec{p}^{\,*}_\omega|}{k^*_\gamma}\left(\mathscr{R}_T + \epsilon_L\,\mathscr{R}_L + \epsilon\,\mathscr{R}_{TT}\,cos(2\phi^*) + \sqrt{2\epsilon_L(1+\epsilon)}\,\mathscr{R}_{TL}\,cos(\phi^*)\right)$$

which connects back to binned experimental data:

$$\left\langle\frac{d^2\sigma_h}{d\Omega^*}\right\rangle_i \simeq \frac{1}{B}\cdot\frac{1}{L\,\langle\Gamma\rangle_i}\cdot\frac{1}{\Delta_i W\,\Delta_i Q^2}\cdot\frac{R_i}{\eta_i}\cdot\frac{N_i}{\Delta_i\Omega^*}$$

i = label of 4D bin
N = background-subtracted yield
B = 3π decay branching ratio
L = integrated luminosity
Γ = virtual photon flux
R = radiative corrections
η = represents effect of all efficiency and acceptance factors

The CLAS Detector

CLAS — CEBAF Large Acceptance Spectrometer
CEBAF — Continuous Electron Beam Accelerator Facility

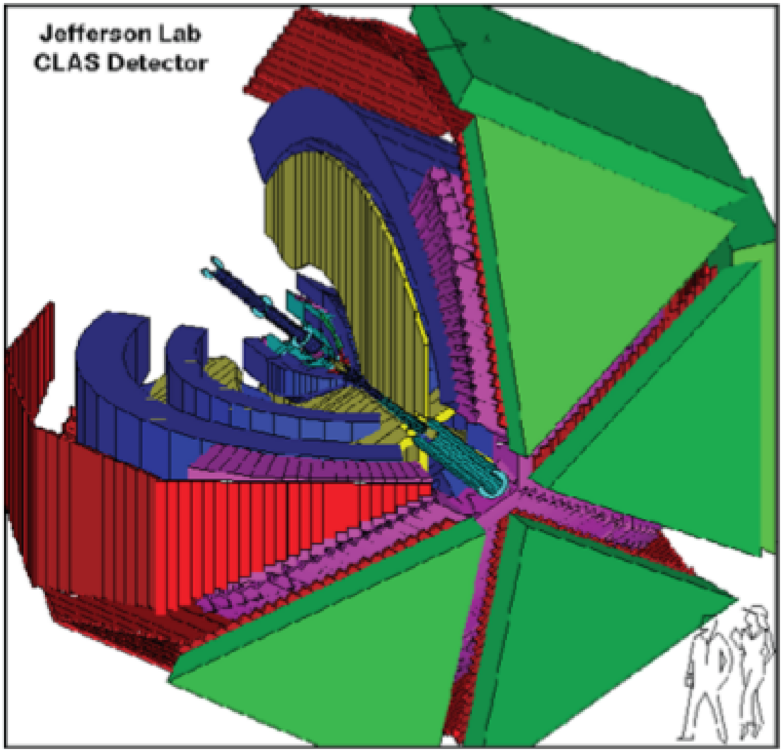

Main Components

- Toroidal Magnet
- Drift Chambers (DC)
- Cerenkov Counter (CC)
- Electromagnetic Calorimeter (EC)
- Time-of-Flight Detectors (TOF)

Experimental conditions

- JLab CEBAF and CLAS detector
- E1F (E16) run periods
- 5-cm unpolarized liquid H target
- target offset by -25 cm (-5 cm)
- 5.5-GeV (5.8-GeV) electrons
- 21-fb^{-1} (28-fb^{-1}) integrated luminosity
- data acquisition triggered by coincident, same-sector hits in Electromagnetic (EC) Calorimeter and Čerenkov Counter CC)

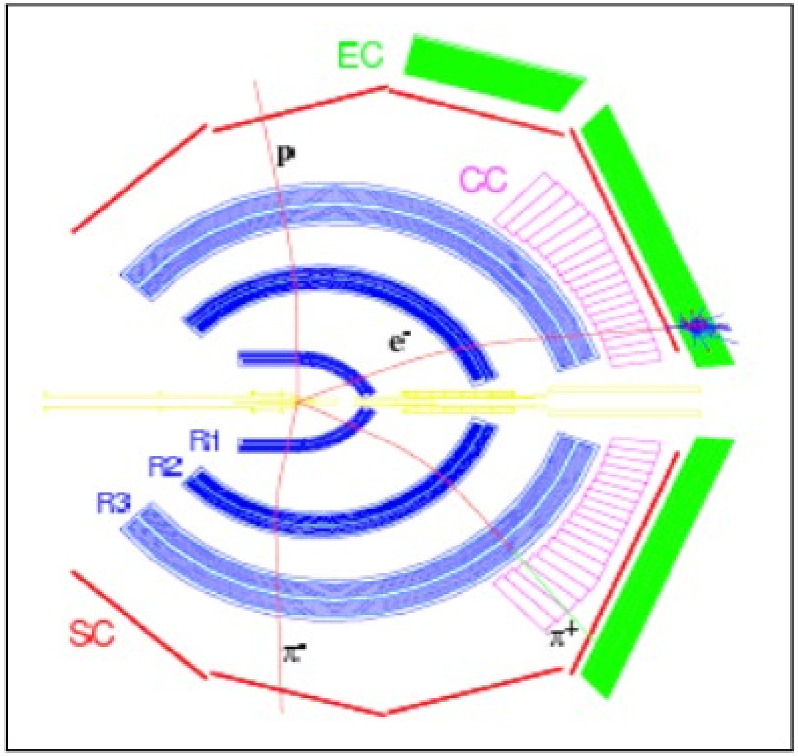

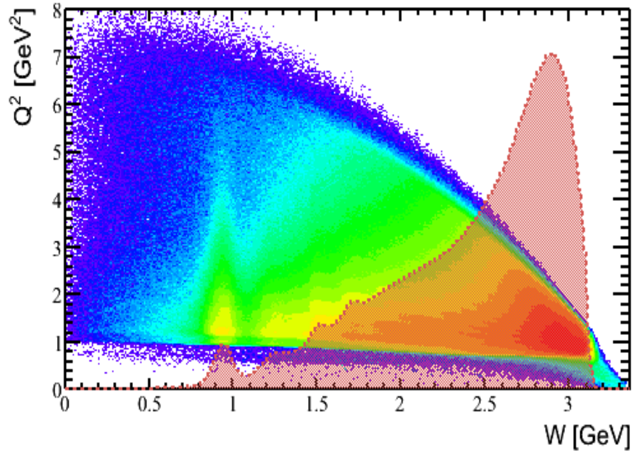

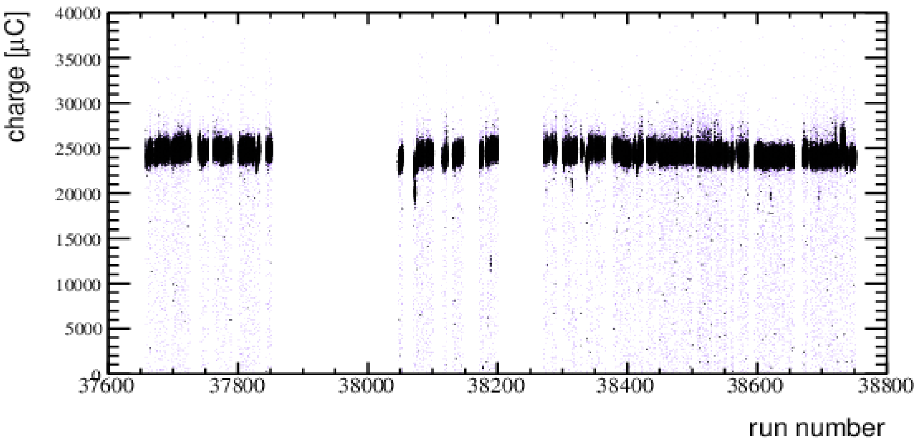

Experimental conditions

- JLab CEBAF and CLAS detector
- E1F (E16) run periods
- 5-cm unpolarized liquid H target
- target offset by -25 cm (-5 cm)
- 5.5-GeV (5.8-GeV) electrons
- 21-fb^{-1} (28-fb^{-1}) integrated luminosity
- data acquisition triggered by coincident, same-sector hits in Electromagnetic (EC) Calorimeter and Čerenkov Counter CC)

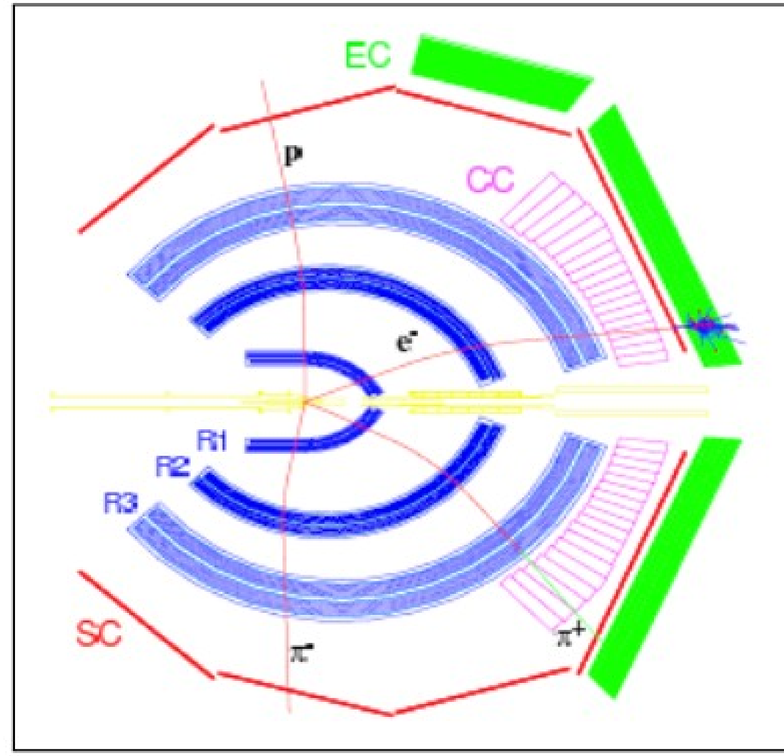

Run and Luminosity Block Quality

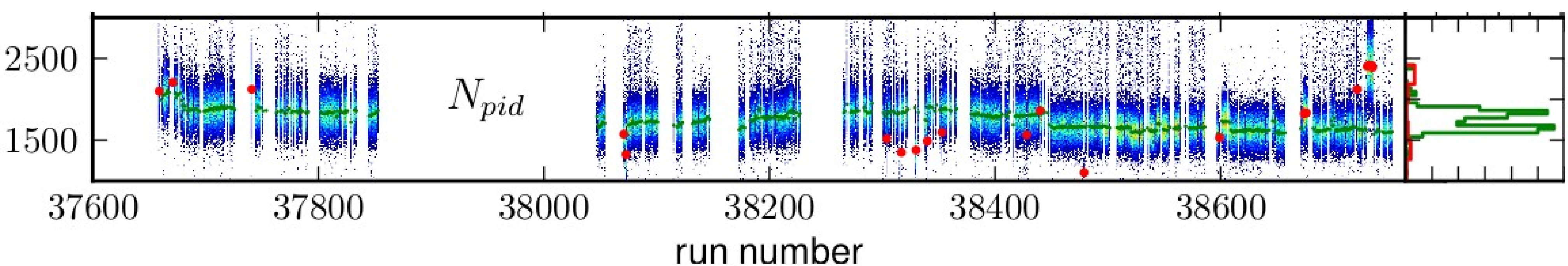

Electron Identification

- **Candidate electron criteria**
  - Same-sector, coincident hits in CC, EC, DC, and SC
  - Geometrically consistent, negative particle track in DC
- **EC-related cuts**
  - E_{EC}/p within 3σ of the EC's sampling fraction
  - E_{in} greater than that of minimum-ionizing particles
- **CC-related cuts**
  - Eliminate low current noise and effect of fast hadrons
  - Determine cut efficiency

$$p_{min} = 214 + 2.47 \times EC_{threshold}$$

$$\sum_{i=0}^{3} a_i p^i < \frac{E_{EC}}{p} < \sum_{i=0}^{3} b_i p^i$$

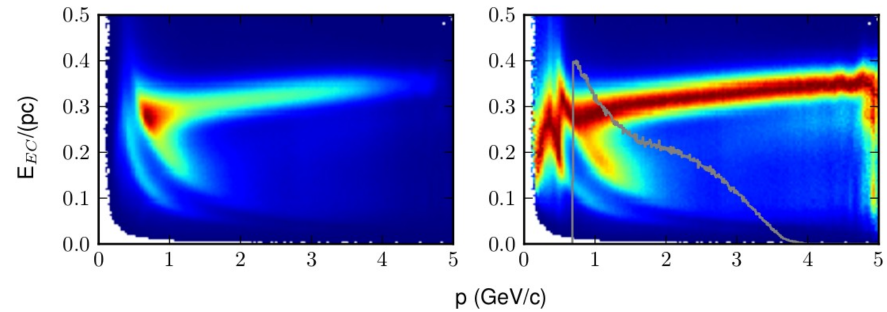

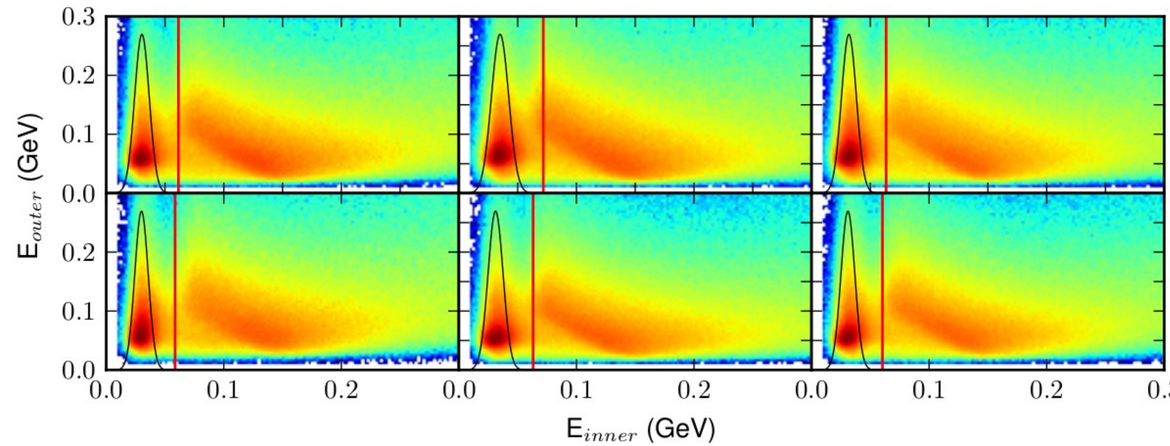

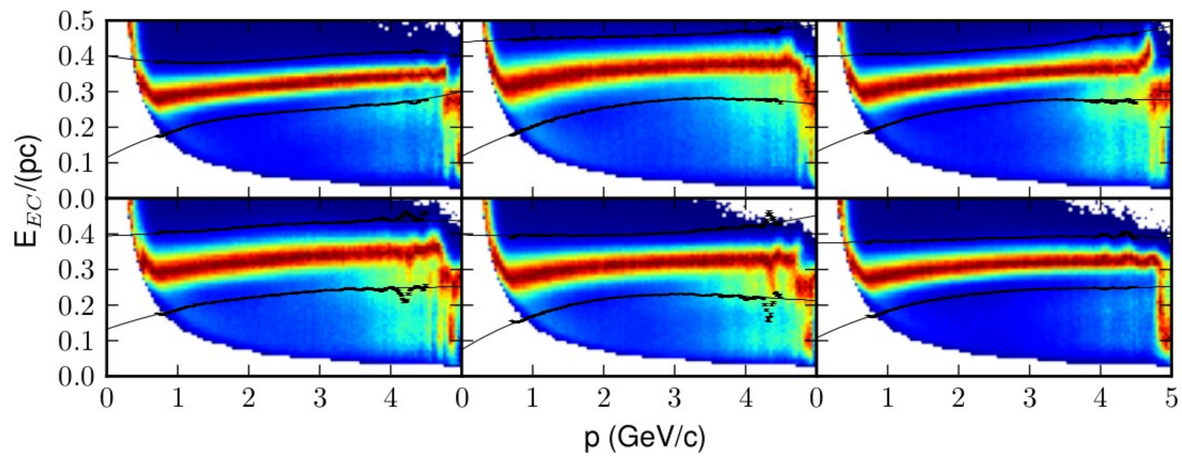

Electron Identification

- **Candidate electron criteria**
  - Same-sector, coincident hits in CC, EC, DC, and SC
  - Geometrically consistent, negative particle track in DC
- **EC-related cuts**
  - E_{EC}/p within 3σ of the EC's sampling fraction
  - E_{in} greater than that of minimum-ionizing particles
- **CC-related cuts**
  - Eliminate low current noise and effect of fast hadrons
  - Determine cut efficiency

$$Noise(x; A, \mu, \sigma, \lambda, B, \tau) + F(x; A_p, \mu_p, \sigma_p)$$

$$\eta_{cc} = \frac{\int_{x_0}^{\infty} F(x)dx}{\int_{0}^{\infty} F(x)dx}$$

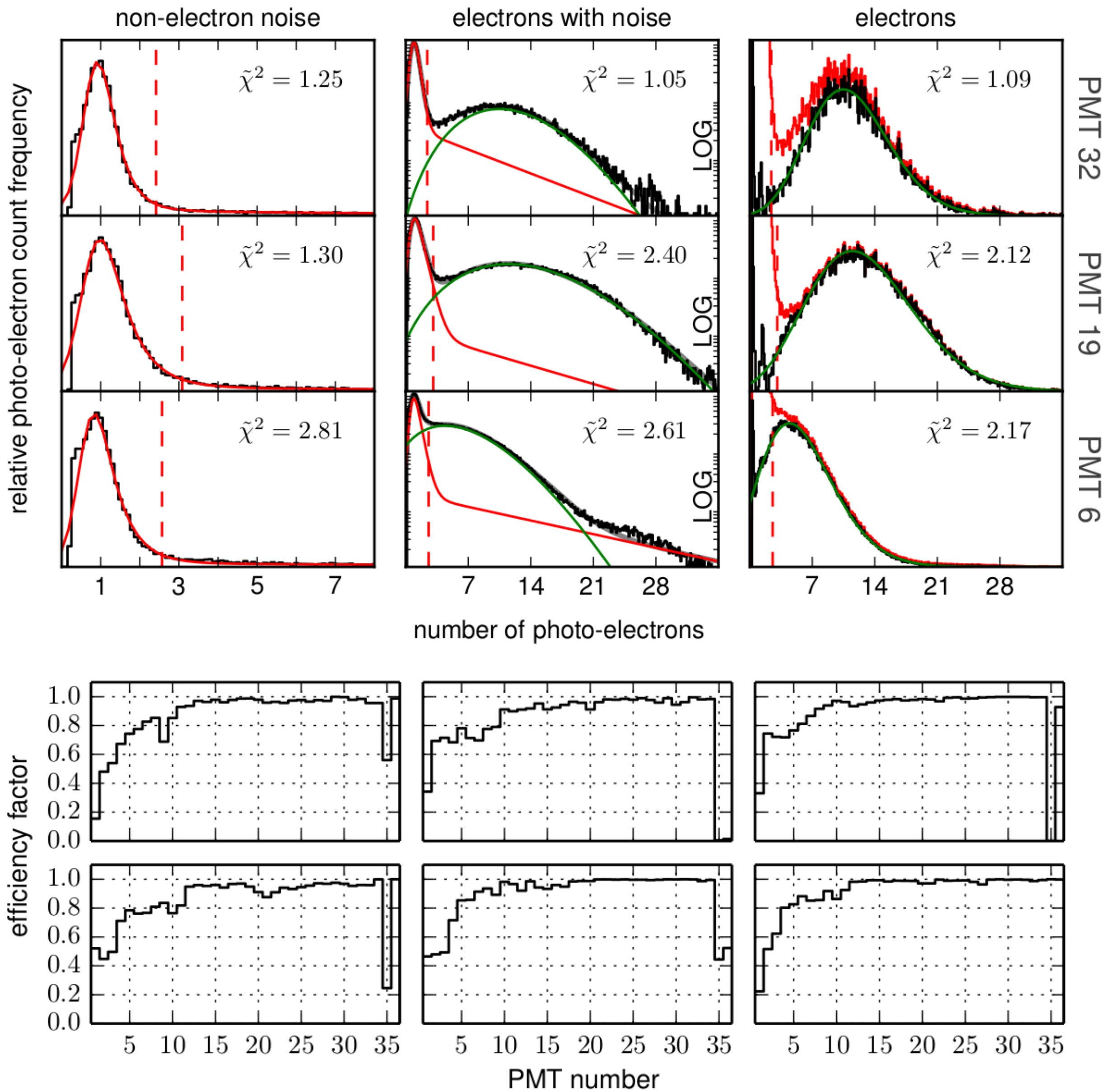

Hadron Identification

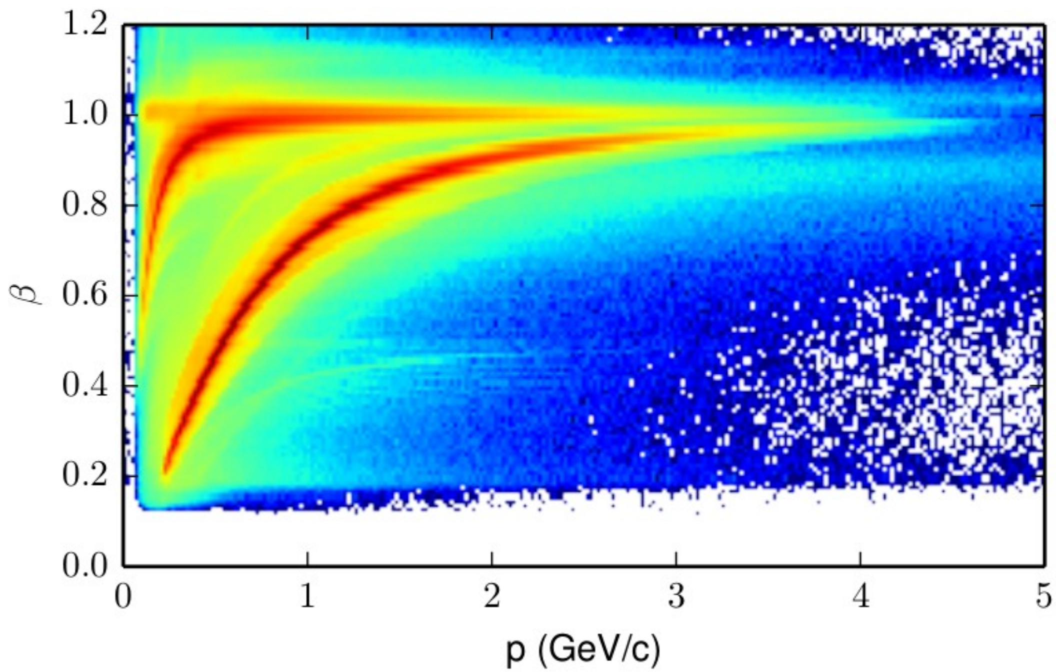

- **Candidate criteria**
  - Same-sector, coincident hits in DC and SC
  - Geometrically consistent, positive particle track in DC
- **Event time correction**
- **Time difference cut**
  - Compare time-of-flight to time predicted by DC-determined momentum with mass assumption.
  - 3σ cut around resulting distribution

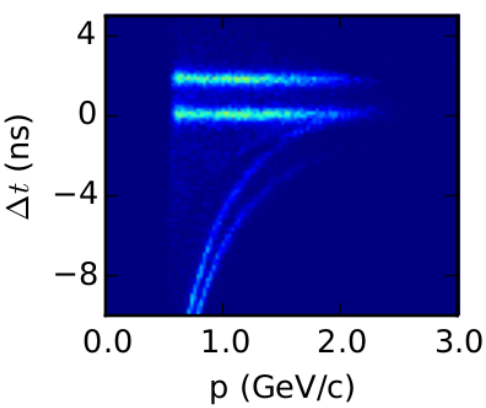

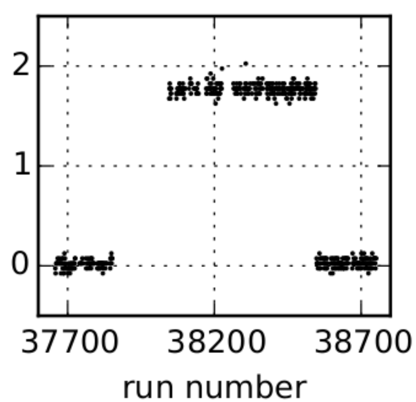

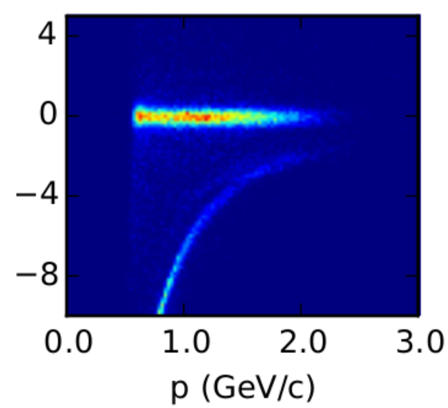

$$t_{TOF} - t_{DC} = (t_{SC} - t_0) - \frac{d_{DC}}{\tilde{\beta} c}$$

$$\tilde{\beta} = \frac{\tilde{v}}{c} = \frac{p}{\sqrt{p^2 + \tilde{m}^2}}$$

Hadron Identification

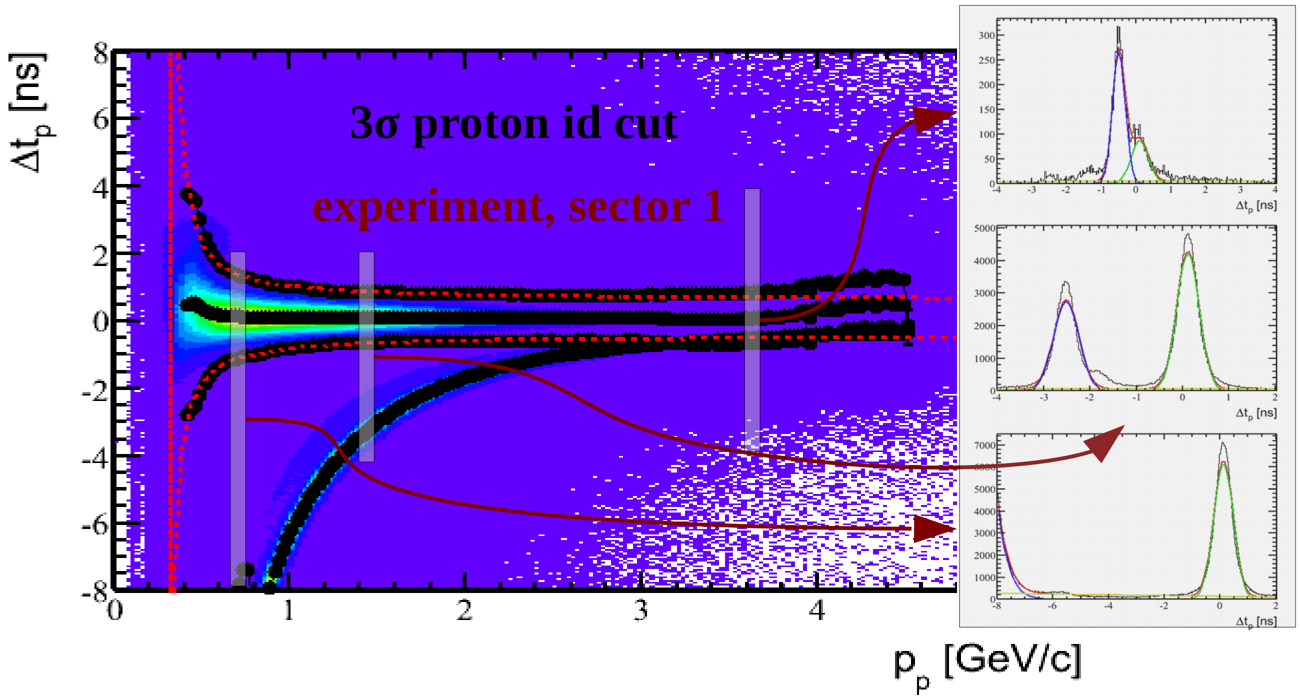

- **Candidate criteria**
  - Same-sector, coincident hits in DC and SC
  - Geometrically consistent, positive particle track in DC
- **Event time correction**
- **Time difference cut**
  - Compare time-of-flight to time predicted by DC-determined momentum with mass assumption.
  - 3σ cut around resulting distribution

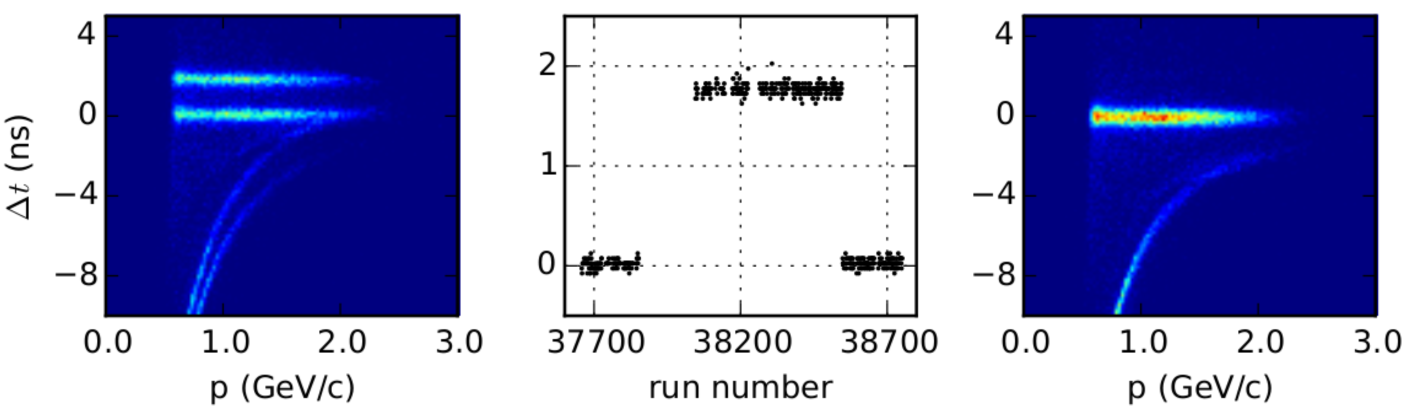

$$t_{TOF} - t_{DC} = (t_{SC} - t_0) - \frac{d_{DC}}{\tilde{\beta} c}$$

$$\tilde{\beta} = \frac{\tilde{v}}{c} = \frac{p}{\sqrt{p^2 + \tilde{m}^2}}$$

Determination of Yield

- **Foundational skim**
  - run is good
  - luminosity block is good
  - first particle is electron
  - exactly 1 proton
  - exactly 1 positive pion
  - up to 1 negative pion
  - no other charged particles
- **Kinematic cuts**
  - $MM_x(epX)$ near ω mass
  - $Mm_x(ep\pi^+X)$ consistent with 3π channel
- **Background subtraction**
  - angular distribution of background sidebands

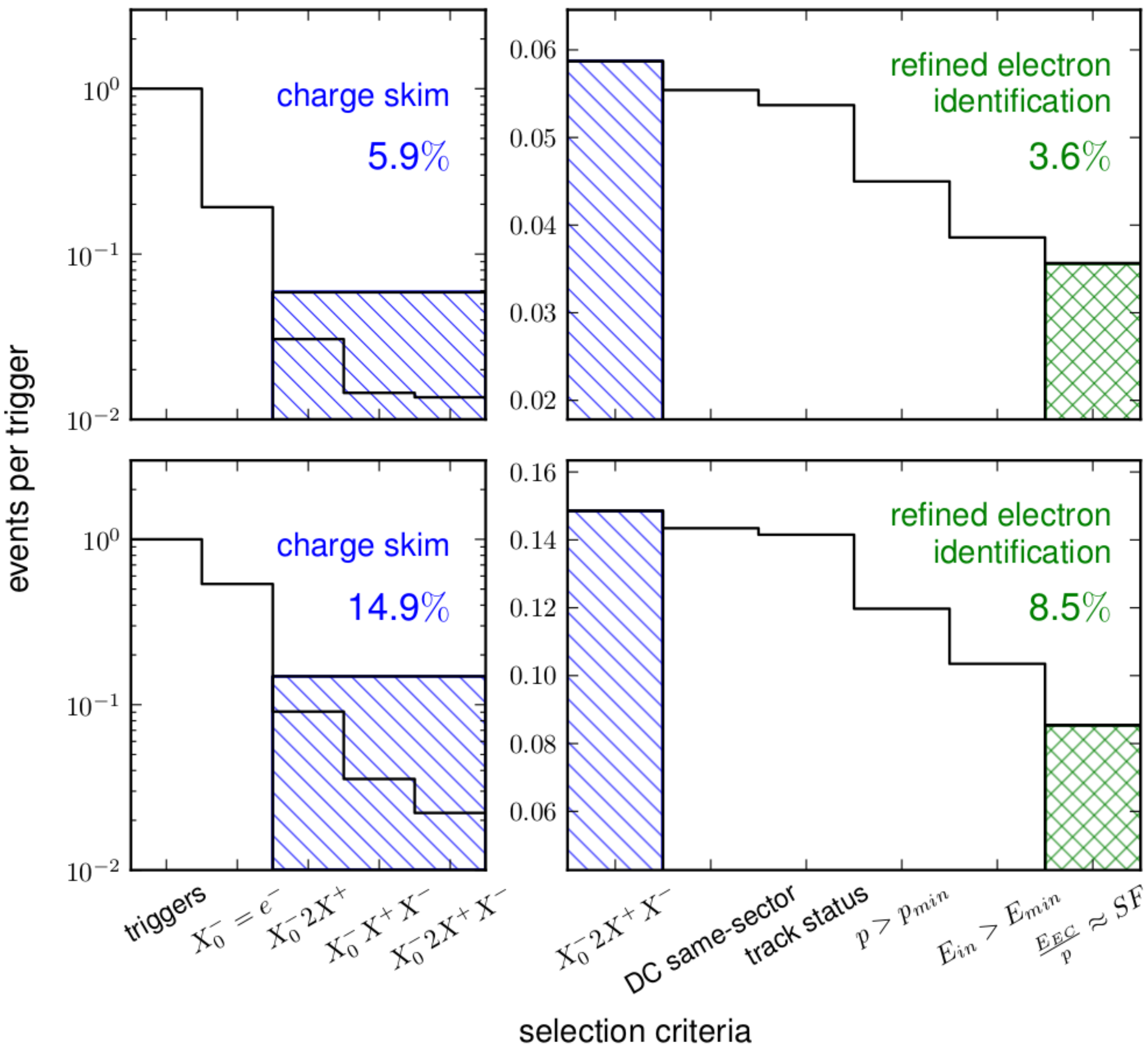

Determination of Yield

- **Foundational skim**
  - run is good
  - luminosity block is good
  - first particle is electron
  - exactly 1 proton
  - exactly 1 positive pion
  - up to 1 negative pion
  - no other charged particles
- **Kinematic cuts**
  - $MM_x(epX)$ near ω mass
  - $Mm_x(ep\pi^+X)$ consistent with 3π channel
- **Background subtraction**
  - angular distribution of background sidebands

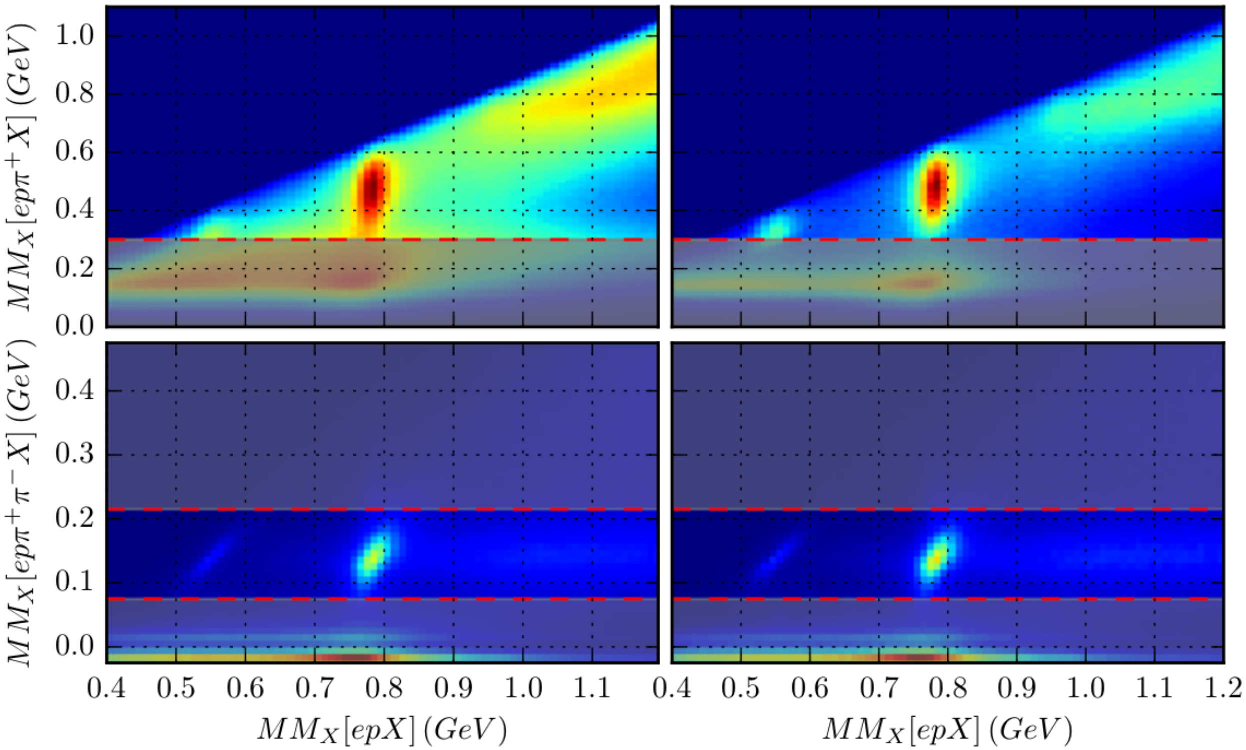

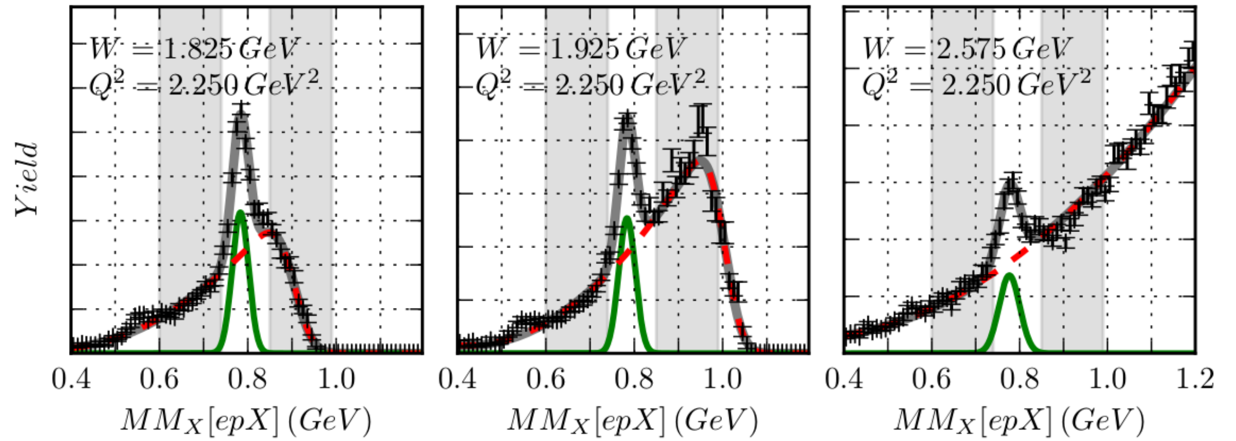

Determination of Yield

- **Foundational skim**
  - run is good
  - luminosity block is good
  - first particle is electron
  - exactly 1 proton
  - exactly 1 positive pion
  - up to 1 negative pion
  - no other charged particles
- **Kinematic cuts**
  - $MM_x(epX)$ near ω mass
  - $Mm_x(ep\pi^+X)$ consistent with 3π channel
- **Background subtraction**
  - angular distribution of background sidebands

$$f(x;a,b,A,\mu,\sigma,p_0,p_1,p_2) = \left(1 - erf\left(\frac{x-a}{b}\right)\right)\cdot\left(Ae^{-\frac{(x-\mu)^2}{2\sigma^2}} + \sum_{i=0}^{2} p_i x^i\right)$$

$$f^{sig} = f(x;a,b,A,\mu,\sigma,0,0,0)$$

$$f^{bg} = f(x;a,b,0,0,0,p_0,p_1,p_2)$$

$$N_\omega^{(2)} = N_{SIG}^{(2)} - \left(\frac{\sum\limits_{j\in SIG} f^{bg}(x_j)}{\sum\limits_{\substack{j\in SB1\\ \cup SB2}} Y_j}\right)\cdot\left(N_{SB1}^{(2)} + N_{SB2}^{(2)}\right)$$

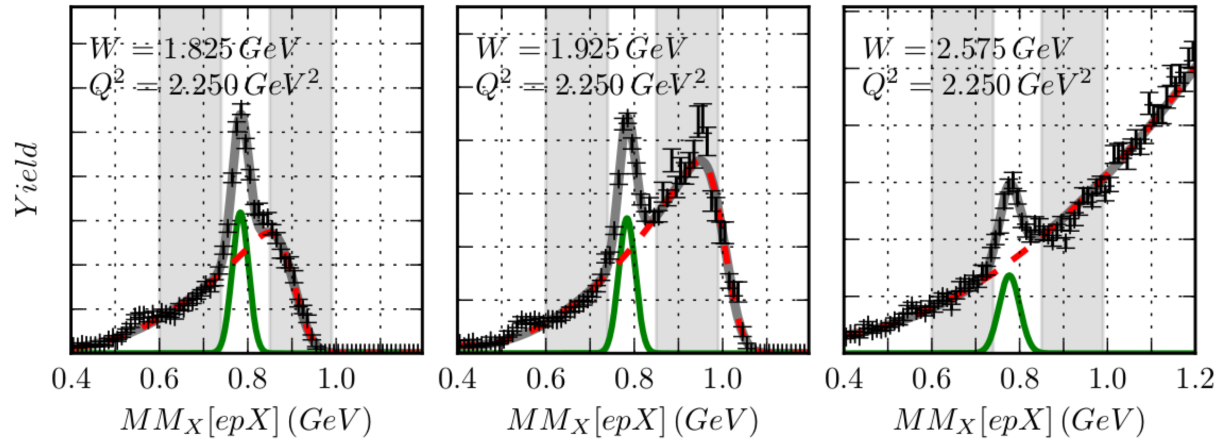

Simulation and Acceptance

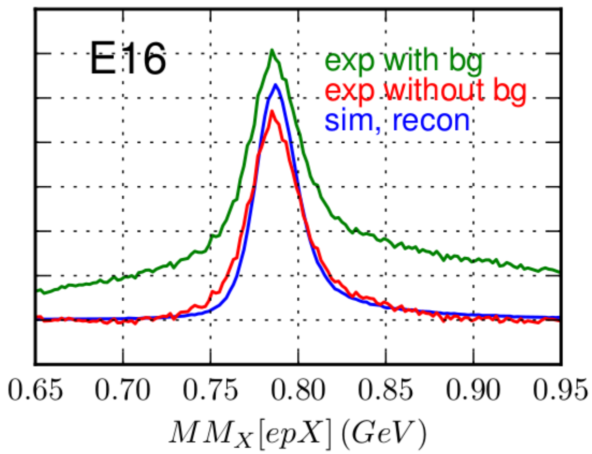

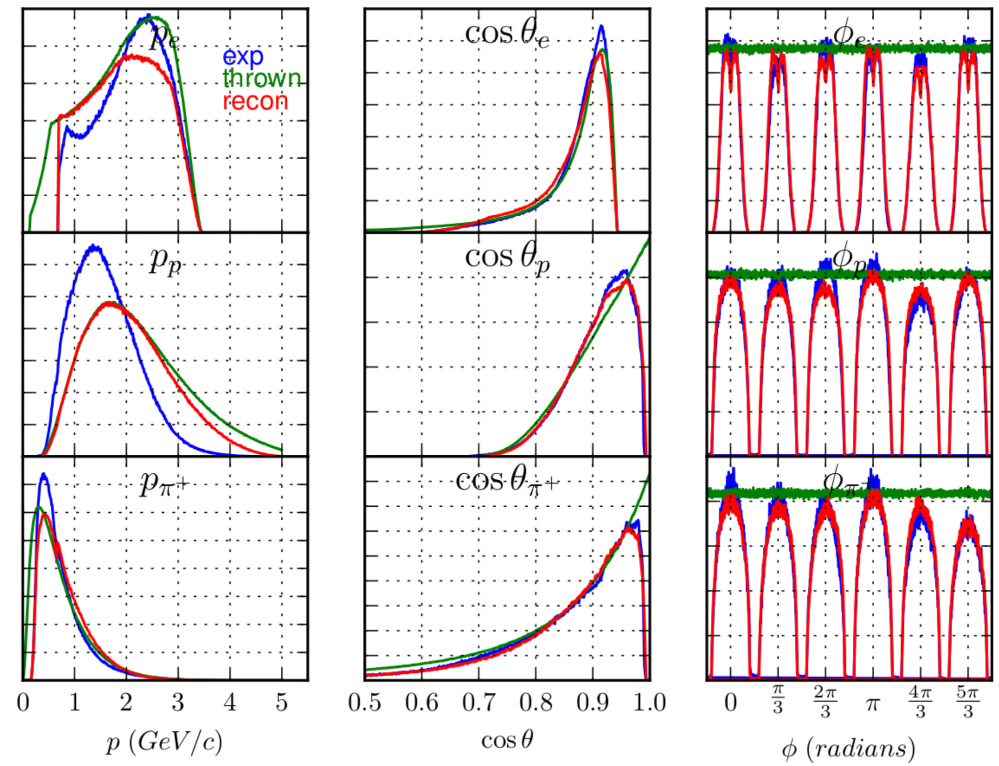

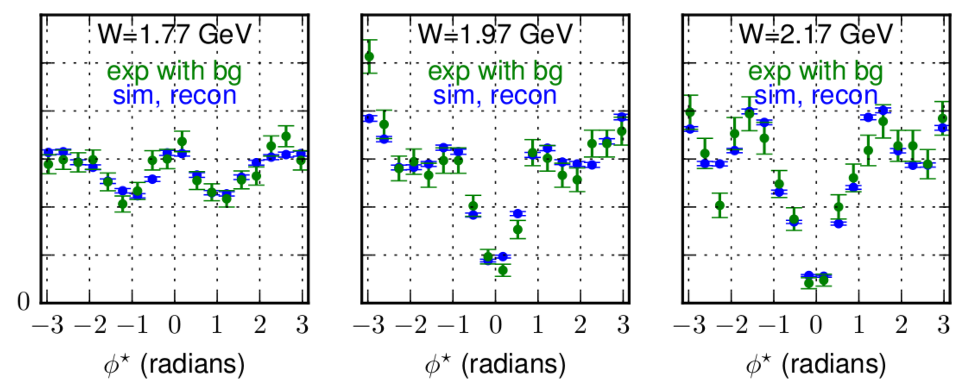

- **Probability to detect/reconstruct**
  - geometric acceptance
  - detector efficiencies
  - reconstruction efficiencies
  - bin migration effects
- GENEV – physics generator
- GSIM – detector simulation
- GPP – additional resolution smearing
- Same reconstruction and cuts as experiment

Simulation and Acceptance

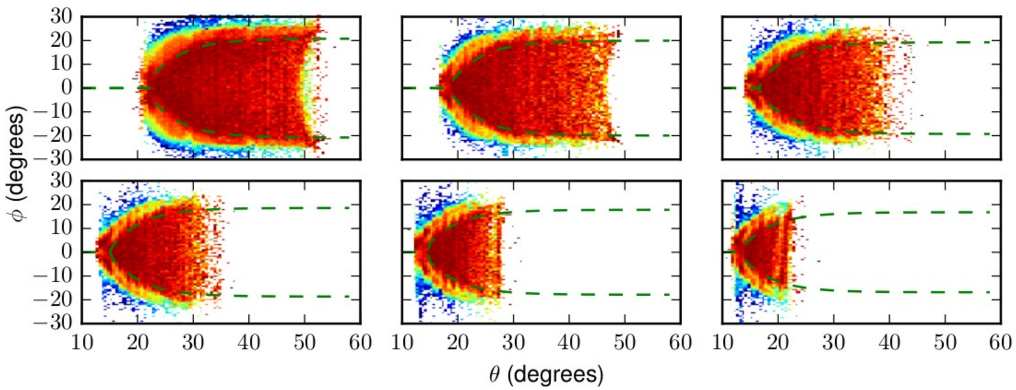

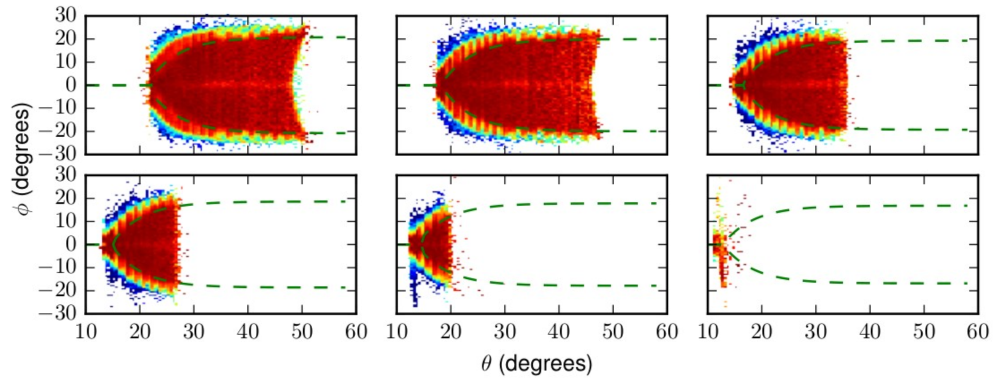

- **Probability to detect/reconstruct**
  - geometric acceptance
  - detector efficiencies
  - reconstruction efficiencies
  - bin migration effects
- GENEV – physics generator
- GSIM – detector simulation
- GPP – addition resolution smearing
- Same reconstruction and cuts as experiment

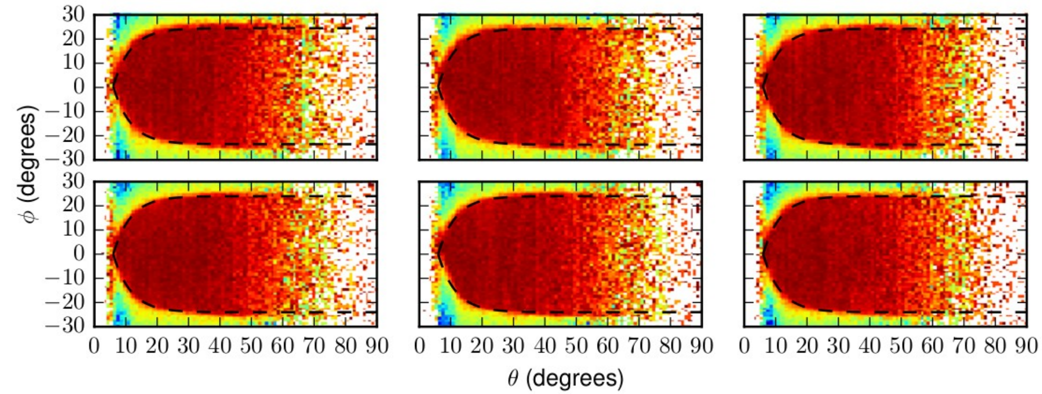

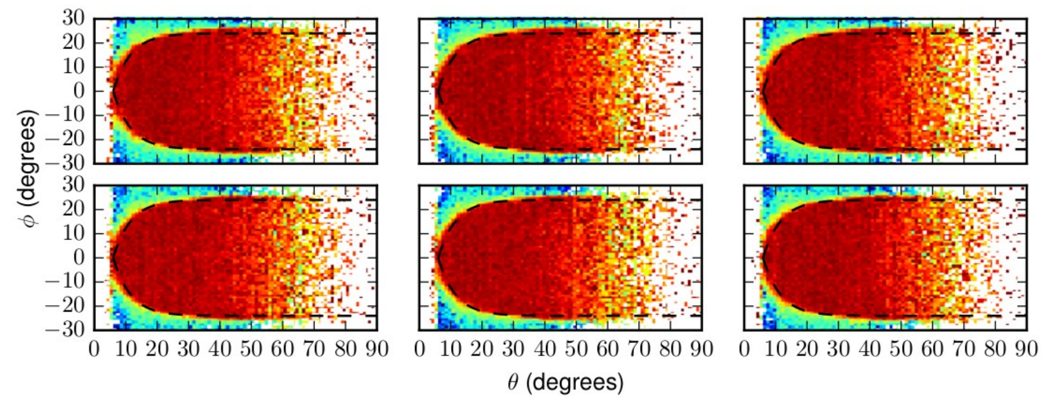

Simulation and Acceptance

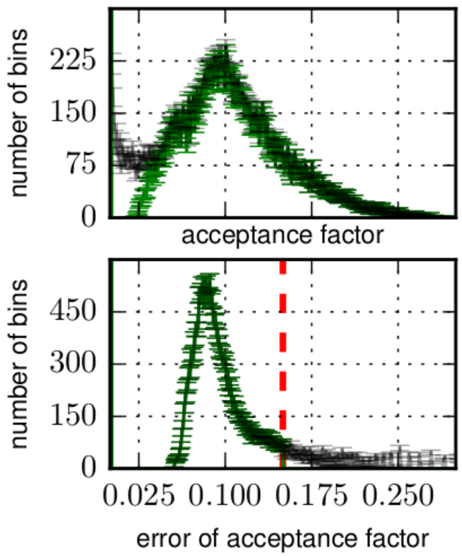

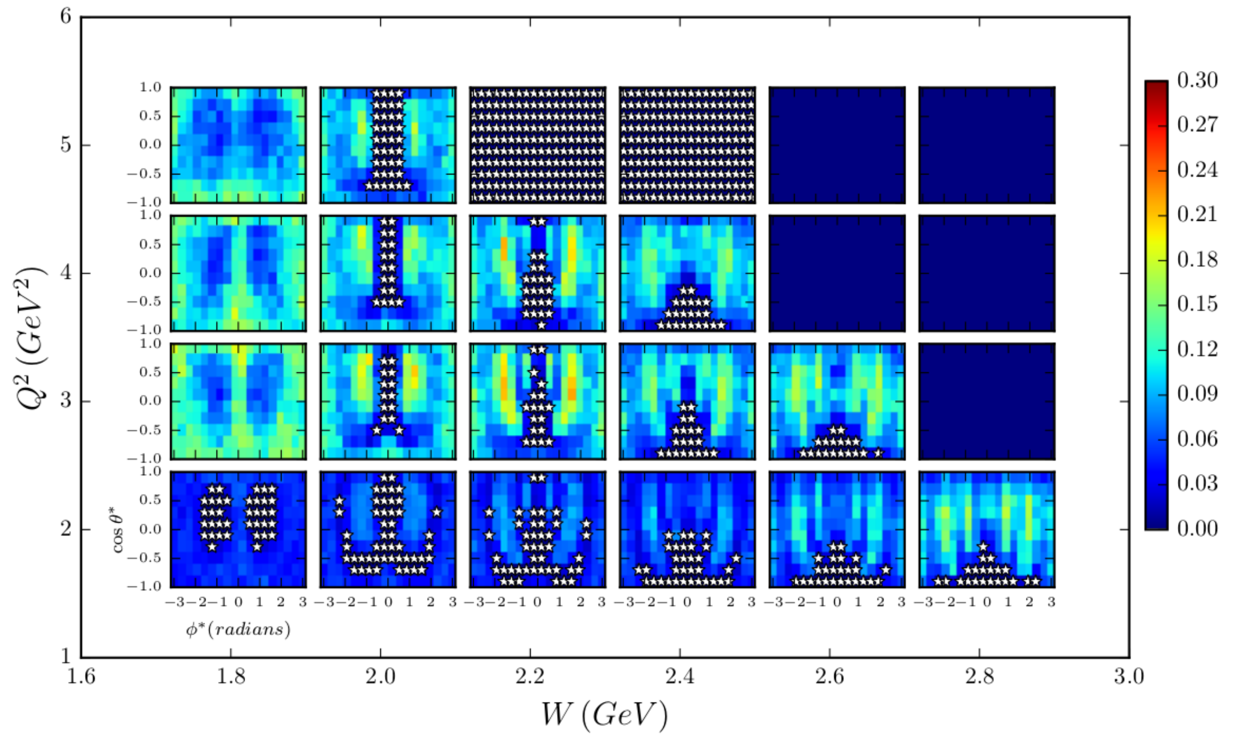

- **Probability to detect/reconstruct**
  - geometric acceptance
  - detector efficiencies
  - reconstruction efficiencies
  - bin migration effects
- GENEV – physics generator
- GSIM – detector simulation
- GPP – addition resolution smearing
- Same reconstruction and cuts as experiment

Events thrown in 82,620 kinematic bins
Events reconstructed in 67,747 kinematic bins

<u>ACCEPTANCE</u> = reconstructed divided by thrown
HOLES = bins WITH thrown
but WITHOUT reconstructed

Other correction factors

- **Radiative correction (Mo and Tsai)**
  - Acceptance corrections account for radiative tail in ω mass peak.
  - Bin migration in W and Q^2 treated separately.
- **E1F reconstruction inefficiency**
  - Raw data requires recooking.
  - Absolute efficiency factor of **0.7** based on recooking of one run
- **Overall reconstruction efficiency**
  - GSIM-CLAS efficiency incongruence

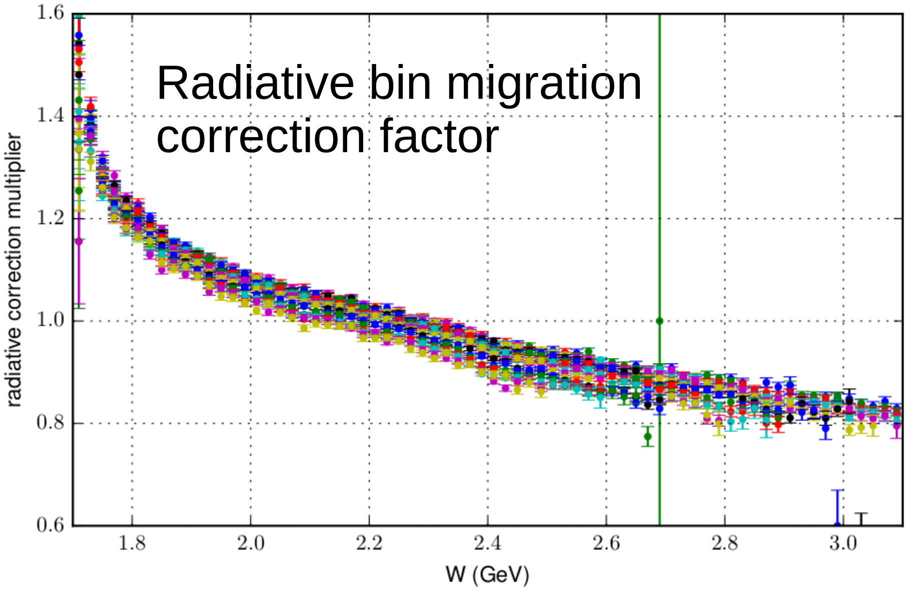

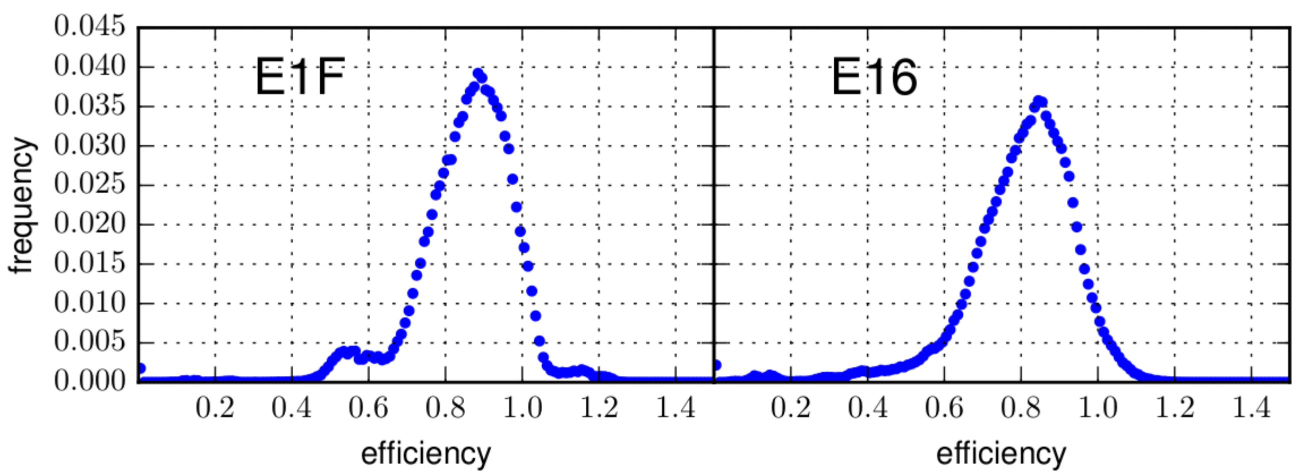

Frequency of event-level “overall reconstruction efficiency” values

Results

1. **Differential cross sections** in more than 60,000 kinematic bins

$$\left(\frac{d^2\sigma_h}{d\Omega^*}\right)_{ijkl} = \frac{1}{\epsilon^{ABS}} \cdot \frac{1}{B} \cdot \frac{1}{L} \cdot \frac{1}{\Gamma_{ij}} \cdot \frac{R_{ij}}{\eta^{ACC}_{ijkl} \left\langle \eta^{CC} \right\rangle_{ijkl} \left\langle \eta^{TR} \right\rangle_{ijkl}} \cdot \frac{1}{\Delta_i W \Delta_j Q^2} \cdot \frac{N_{ijkl}}{\Delta_{kl}\Omega^*}$$

2. **Unpolarized cross section**, σ_o, and **interference terms**, σ_{TT}, and σ_{LT}

$$\frac{d\sigma_h}{d\phi^*} = \frac{1}{2\pi}\left(\sigma_o + \epsilon\,\sigma_{TT}\,cos(2\phi^*) + \sqrt{2\epsilon(1+\epsilon)}\,\sigma_{LT}\,cos(\phi^*)\right)$$

3. **Response functions**, $\mathscr{R}_T + \epsilon_L \mathscr{R}_L$, $\mathscr{R}_{TT}$, and $\mathscr{R}_{TL}$

$$\frac{d^2\sigma_h}{d\Omega^*} = \frac{|\vec{p}^{\,*}_\omega|}{k^*_\gamma}\left(\mathscr{R}_T + \epsilon_L\,\mathscr{R}_L + \epsilon\,\mathscr{R}_{TT}\,cos(2\phi^*) + \sqrt{2\epsilon_L(1+\epsilon)}\,\mathscr{R}_{TL}\,cos(\phi^*)\right)$$

Results

$$\frac{d\sigma_h}{d\phi^*} = \frac{1}{2\pi}\left(\underline{\sigma_o} + \epsilon\,\sigma_{TT}\,cos(2\phi^*) + \sqrt{2\epsilon(1+\epsilon)}\,\sigma_{LT}\,cos(\phi^*)\right)$$

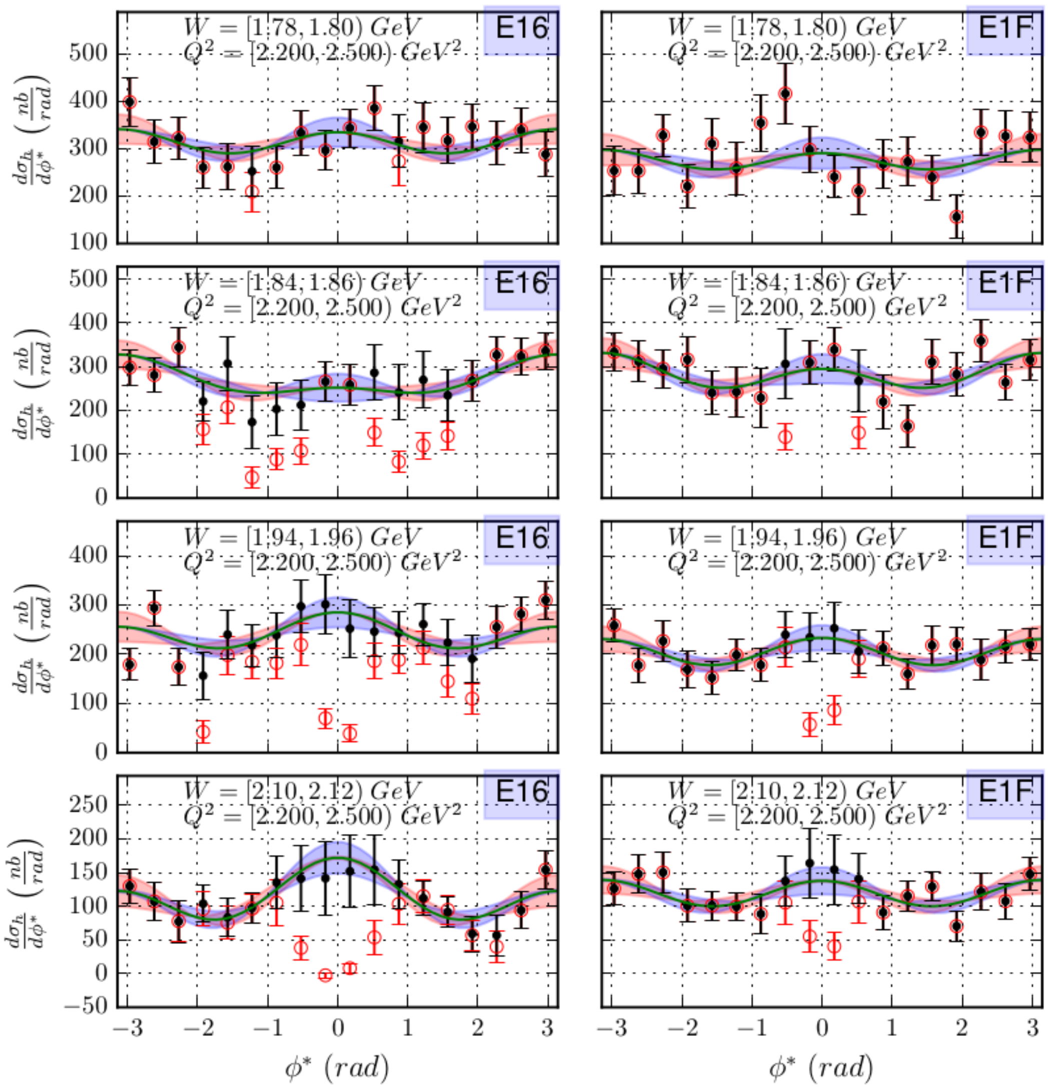

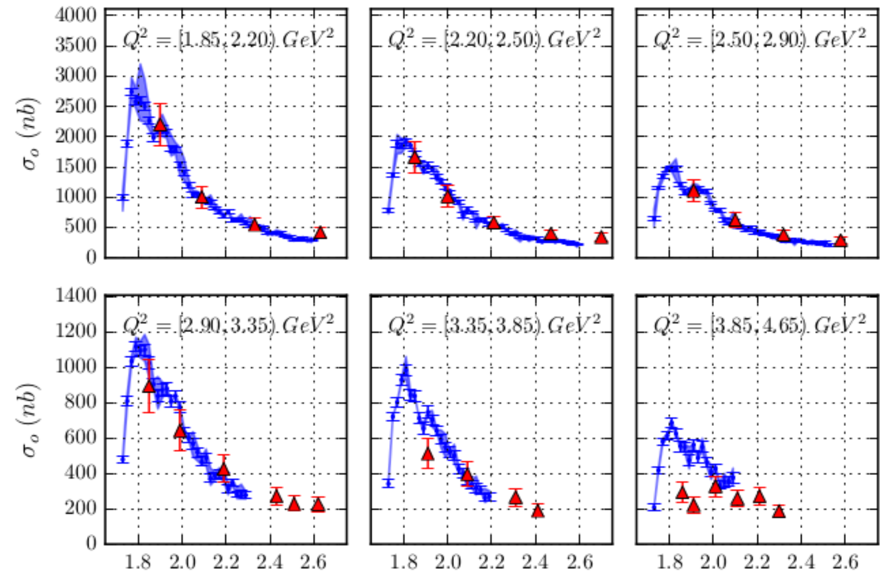

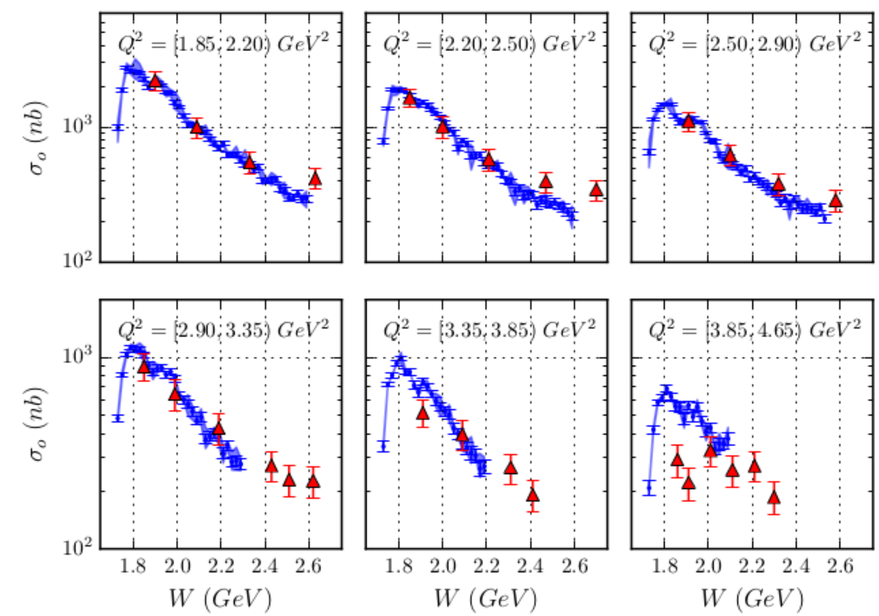

Results

$$\frac{d\sigma_h}{d\phi^*} = \frac{1}{2\pi}\left(\sigma_o + \epsilon\,\underline{\sigma_{TT}}\,cos(2\phi^*) + \sqrt{2\epsilon(1+\epsilon)}\,\underline{\sigma_{LT}}\,cos(\phi^*)\right)$$

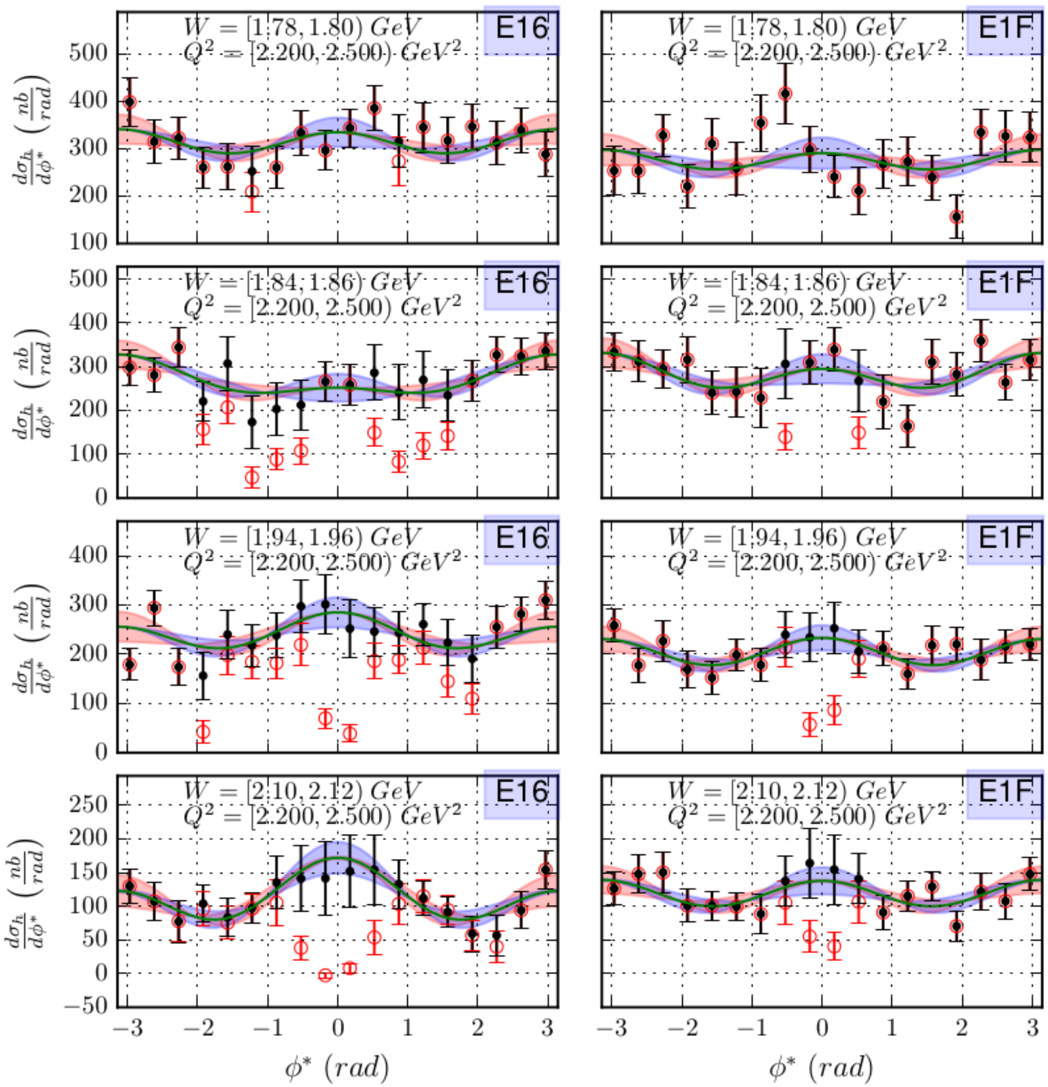

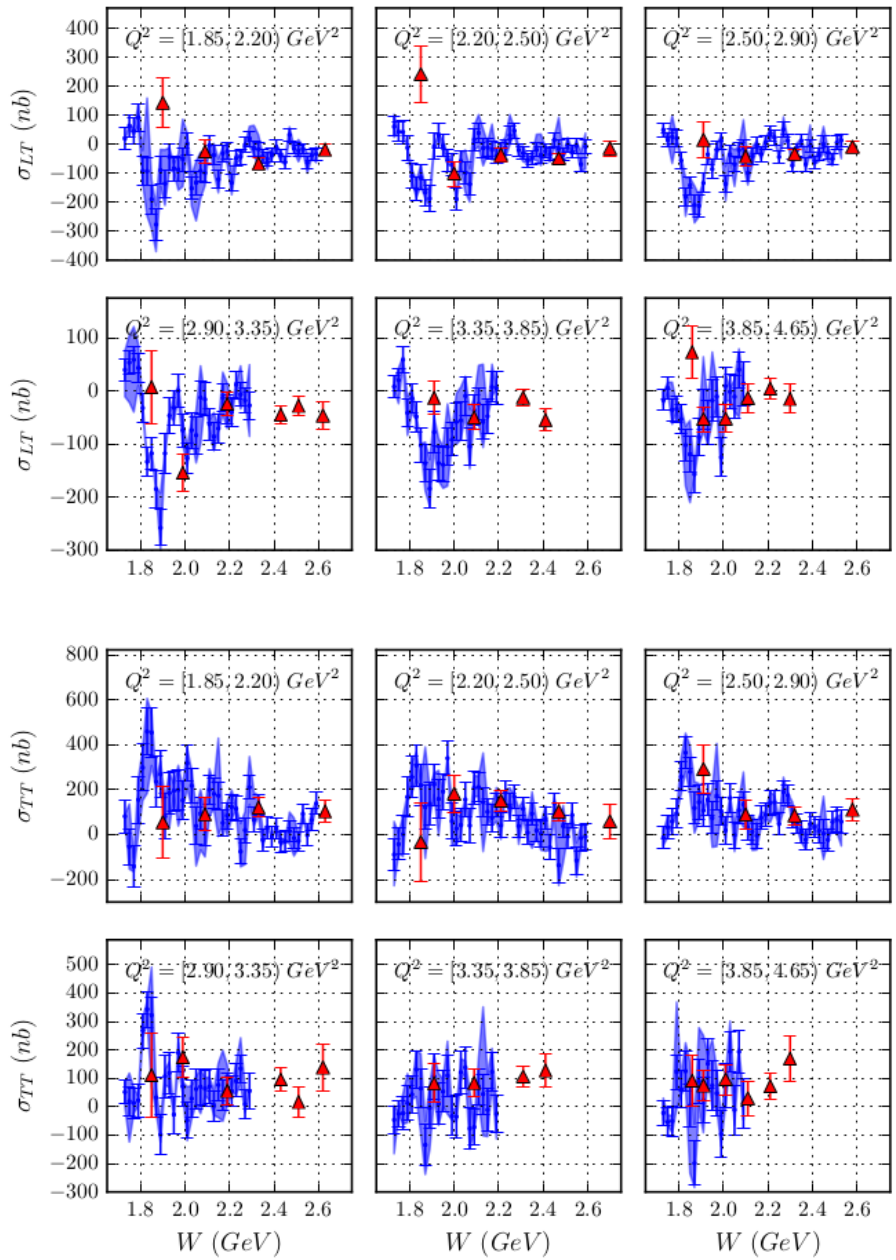

Results

$$\frac{d^2\sigma_h}{d\Omega^*} = \frac{|\vec{p}^{\,*}_{\omega}|}{k^*_{\gamma}} \left(\underline{\mathscr{R}_T + \epsilon_L\,\mathscr{R}_L} + \epsilon\,\underline{\mathscr{R}_{TT}}\,cos(2\phi^*) + \sqrt{2\epsilon_L(1+\epsilon)}\,\underline{\mathscr{R}_{TL}}\,cos(\phi^*) \right)$$

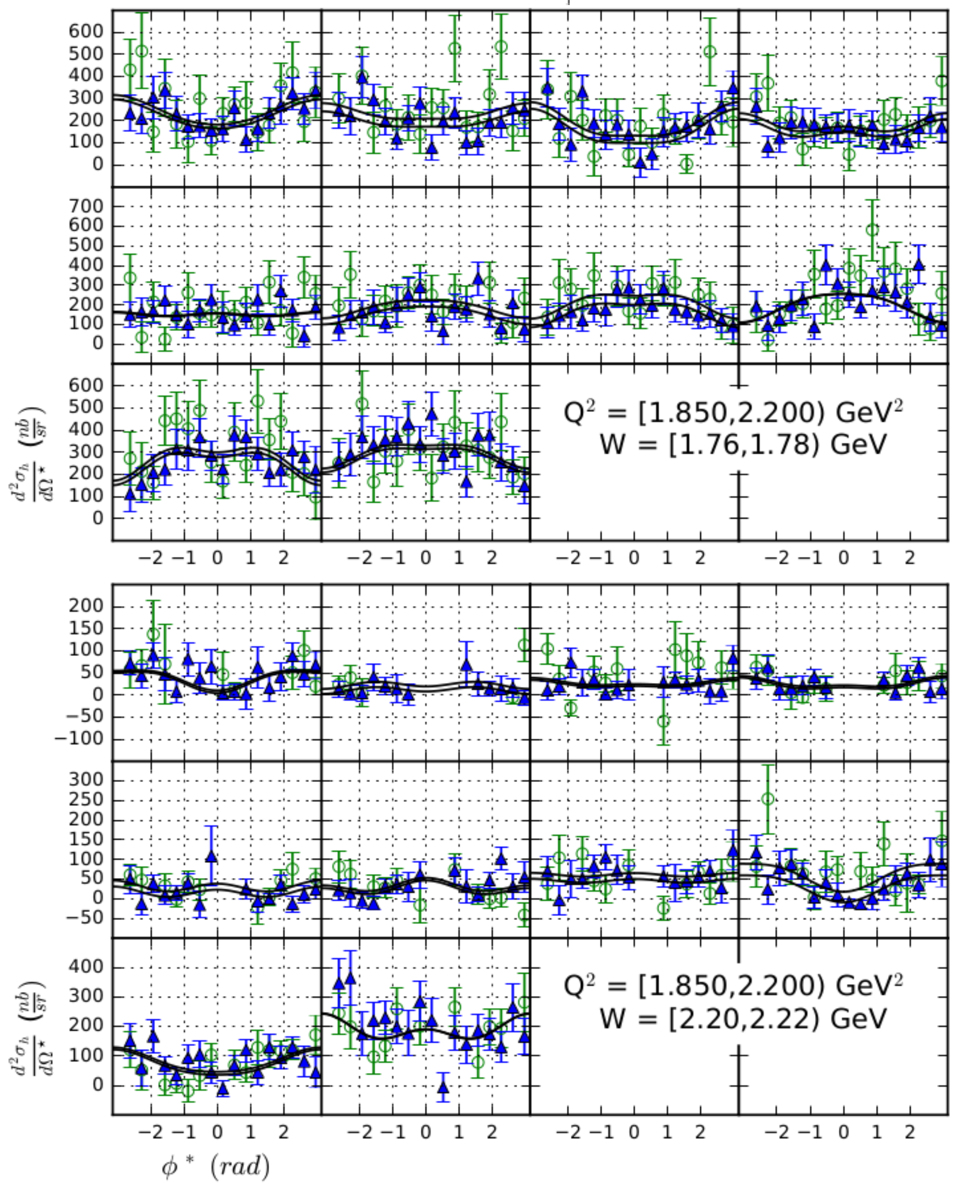

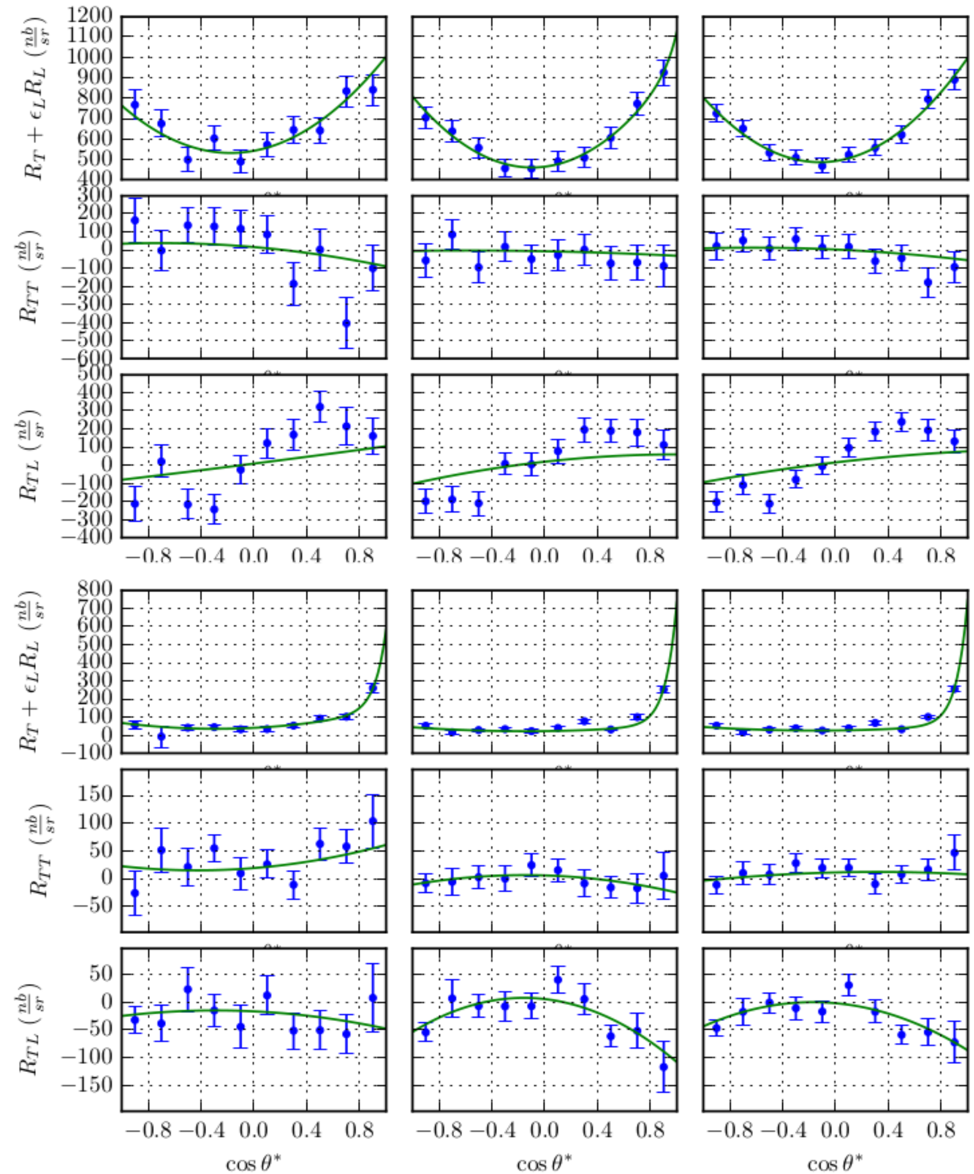

Results

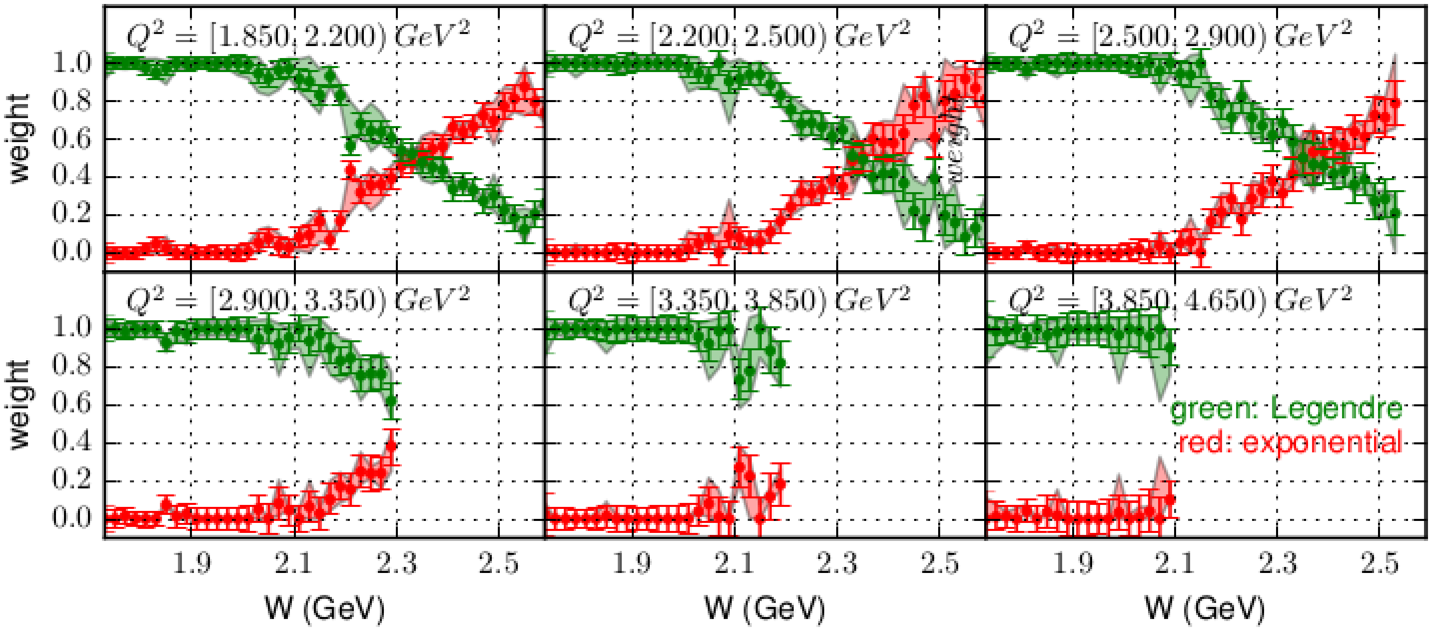

Figure 7.8 Relative Legendre and exponential weight factors evolve with W. These are the weight factors required to model $\mathscr{R}_T + \epsilon_L \mathscr{R}_L$ as a function of θ^*. At low-W, second-order Legendre polynomials match well with the response functions shape in θ^* (green points are close to 1). As W increases and t-channel processes become accessible, the exponential is required to strengthen weight to reflect the forward-peaking nature of t-channel processes (red points are increasing from 0).

Highlights

• Response functions $R_T + \varepsilon R_L$, R_{TT}, and R_{TL} were extracted in the kinematic range covered by W = [1.72, 2.60) GeV and Q^2 = [1.85, 5.15) GeV^2.

• Combined analysis of E1F and E16 run periods presents the **largest set of results for ω electroproduction** in the resonance region to date. Far more structure in W is apparent than in prior results, due to increased precision afforded by higher statistics.

• **Most precise angular information** on ω electroproduction in the virtual photon domain. Intended to support single- and coupled-channel analyses that aim to probe the content and dynamics of hadrons.

• **Cross-sections are relatively flat in θ up to W = 2.1 GeV.** Only at higher energies does the onset of forward-angle dominance suggestive of t-channel processes occur.

• Unpolarized cross-sections are inconsistent with previously published E16 results at the highest common Q^2 values.

Thank you!